

# Preliminary neutronic assessments for the development of the VIS/IR diagnostic systems located in the ITER EPP

Iole Palermo<sup>1\*</sup>, Fernando Mota<sup>1</sup>, Luis Rios<sup>1</sup>, Juan Pablo Catalán<sup>2</sup>, Javier Alonso<sup>1</sup>, Angel Ibarra<sup>1</sup>

<sup>1</sup>CIEMAT, Fusion National Laboratory, Av. Complutense 40, E-28040 Madrid, Spain

<sup>2</sup>UNED, Dept. of Energy Engineering, c/ Juan del Rosal 12, E-28040 Madrid, Spain

\*Corresponding author email: [iole.palermo@ciemat.es](mailto:iole.palermo@ciemat.es)

## Abstract

The paper focuses on the nuclear analyses of the ITER Equatorial Port Visible/Infrared Wide Angle Viewing System (VIS/IR WAVS). This instrument comprises of viewing systems in the 4 Equatorial Ports (EP) 3, 9, 12 and 17. The main mission of this diagnostic is to support the operation of the tokamak by providing visible and infrared viewing and temperature data of the first wall to protect it from damage. Its design is driven by both the tokamak severe environment and the high performances required for machine protection. New nuclear studies have been carried out for the development of the diagnostic and for test purposes under ITER-like irradiation conditions in order to choose the most appropriate materials for the optical components. Thus, three neutronic analyses have been carried out: the first in order to verify if silver could be used as a covering material for the optical components in different location of the Interspace area; the second in order to establish the irradiation time required in a Co-60 gamma facility (at CIEMAT) for testing purposes of the sapphire vacuum window; and the third to give more detailed specifications for the irradiation campaigns under gamma (in the Co-60 facility) and neutrons (at SCK•CEN BR2 reactor), about the time required to achieve the same dose than the one accumulated in ITER at the end-of-life (EOL) in the different components of the Port area for the materials proposed as substrate and coatings. The neutronic and activation calculations have been performed using the Monte Carlo code MCNP5, the activation code ACAB and the cross section libraries FENDL 2.1 and EAF-2007. The description of the simulations and their results are presented in this paper.

**Keywords:** neutronics, ITER, diagnostics, optical materials

## 1. Introduction

In the framework of the EFDA Goal Oriented Training (GOT) Programme “EFDA-GOT-4-DIAG” in the field of Diagnostic Techniques, the Work Programme 7, started at CIEMAT at the end of 2013, has been focused on the neutronic studies, mechanical design and Port-Plug integration of the ITER Equatorial Port Visible/Infrared Wide Angle Viewing System (VIS/IR WAVS). This paper addresses the preliminary nuclear analyses of the system associated to the choice of materials for the optical components.

The Visible Infrared WAVS is an optical diagnostic intended to be used during plasma operation to provide images of the in-vessel components such as Port Plugs, blankets and divertor. It operates in the visible spectrum (400-700 nm) and also in the infrared wavelengths (3-5  $\mu\text{m}$ ). This instrument will cover a large field of view with high spatial and temporal resolutions, providing real time temperature measurements, spectral data in the visible range, information on runaway electrons, and pellet tracking.

The previously foreseen toroidal distribution of the EP Visible Infrared systems used the equatorial ports 1, 3, 9, and 12 – always at the position of drawer D1 (which is the rightmost drawer looking from the plasma). The description of the previous designs and analyses for the diagnostic components, optical paths, integration in the EP1 and the shielding optimization implemented until the date (through optimization of gaps, dog-legs and labyrinths) can be found in references [1-6].

This arrangement was changed in order to achieve the best coverage while avoiding clashes with other diagnostics requiring the same location. Currently the planned locations for the VIS/IR WAVS are the Equatorial Ports 3, 9, 12 and 17 using the drawer 1 in all of these ports with exception of EP3, where it occupies drawer 3 and basically consists of a mirrored version of the system. Thus, for a wide coverage of the in-vessel components, the system is composed by 4 lines of sight: upper view - looking at the blankets of the upper target; left and right views - tangential views covering all of the equatorial and upper heating ports, some diagnostic ports, most of the outboard and inboard blankets and some areas in the divertor; and divertor view - a larger view looking at the divertor with high resolution. Figure 1a shows the details of the 4 optical paths inside the Port Plug. In the current status of the optical design (CDR design), the systems is comprised of mirrors inside the Port Plug, sapphire windows on the port closure plate, a field lens, a Cassegrain telescope, dichroic filters to split VIS and IR lines, some lenses in the Port Interspace, a dogleg behind the bioshield and more lenses in the Port Cell up to the cameras [7]. Figure 1b shows such details of the diagnostic systems from the first mirror inside the Port Plug to the cameras in the Port Cell.

Many analyses have been already performed [7-9] for this version of the VIS/IR WAVS at Conceptual Design stage but extensive R&D programmes are still ongoing in order to solve the main problems regarding the nuclear effects on the optical materials and in order to obtain a viable Engineering design.

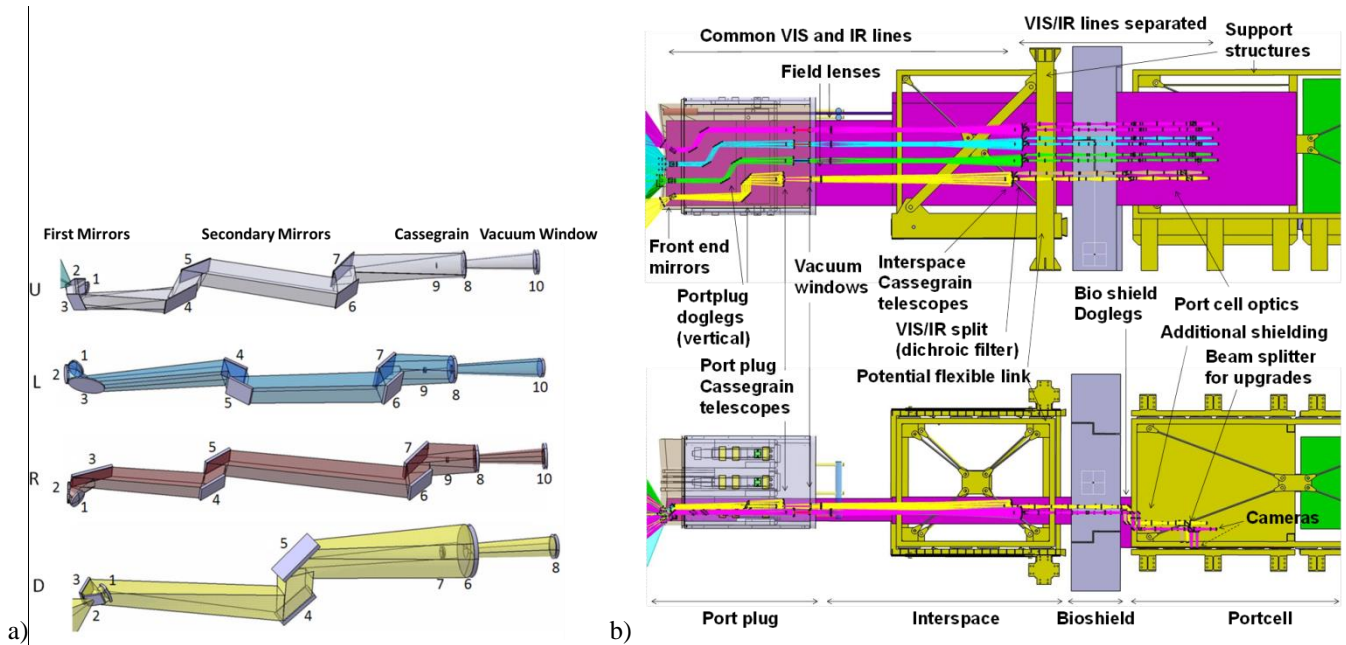


**Figure 1.** a) The VIS/IR optical lines for the four views of the plasma (Upper, Left, Right and Divertor views)[8]; b) current state of the optical design from the Port Plug to the Port Cell showing the components considered until the moment [7].

## 2. Radiation effects on the optics materials

The optical components are expected to maintain their properties under high levels of ionizing radiation (tens to hundreds Gy/s), during many hundreds of hours. In addition some materials will be subjected to atomic displacements of the order of  $10^{-10}$  dpa/s or higher. The main properties of interest (optical absorption, radioluminescence, mechanical properties, etc) are closely related to the presence of defects. The optical windows must also act as confinement barriers for tritium and other radioactive products. In addition, coloring and loss of transparency caused by the irradiation of the optical materials are also concerns. Summarizing, the major effects produced by the nuclear environment in which the optical components will be immersed and which are required to be investigated are: deformation of the optical surface due to nuclear heating, point defects that can act as color centers and therefore produce obscuration of the optics, radioluminescence induced by the ionizing radiation which could generate spurious signal, and loss of mirrors reflectivity due to particles deposition (contaminants e.g. Be, W, Fe) or erosion (energetic particles from plasma).

Due to the known and crucial issue of the radiation effects on the optical components, an assessment of the suitability of possible materials (for both visible and IR lines in different configurations) is being investigated for the different WAVS components:

- Refractive elements (e.g. lenses, dichroic filters and beam-splitters)
- Reflective elements (e.g. metallic periscope mirrors, if necessary)
- Coatings (e.g. anti-reflection for coatings, mirrors, filters and beam-splitters)
- Optical cements (e.g. curing epoxies).

Some authors [10, 11] gave a list of recommended materials for different diagnostic components including windows and mirrors as well as the results of various irradiation tests and the maximum allowable dose or dose rates. Among them, different oxides, mainly fused (amorphous) silica ( $\text{SiO}_2$ ) and aluminium oxide ( $\text{Al}_2\text{O}_3$ ), have been considered as favorite candidate materials for windows and lenses in the diagnostics systems. Nevertheless [12,13] both radiation induced optical absorption and light emission (radioluminescence) impose severe limitations on the use of silica and sapphire, present day ITER candidate materials, making it extremely difficult to separate out the plasma emission from the window emission and absorption [14].

Others materials, in addition to these, have been taken into account in the following analyses, such as Bulk Al alloy, SiC and ULE, as substrate, and Ag and  $\text{Nb}_2\text{O}_5$ , as coatings. Their characteristics as optical components will be mentioned in section 4.

The material assessment activity necessitates the calculation along the whole optical paths of neutron fluxes, doses and dpa, among others. Preliminary neutronic assessments devoted to allow an efficient selection and test of the proposed materials are described in the following sections.

## 3. Methodology

In order to implement the nuclear analyses of the diagnostic here described the following procedure has been employed:

1. First of all the CAD input model of the Equatorial Port Plug (EPP) and of the VIS/IR components occupying the Port area [15] is simplified by means of SpaceClaim Engineer software [16] which allows to reduce the complexity of the engineering models to a level compatible with the geometrical capabilities of the Monte Carlo transport code (simplification of the spline, elimination of little components and unnecessary details, completion of the model filling the void spaces, among others). Apart from the

VIS/IR Wide Angle Viewing System that has been introduced in the drawer 1, the EPP used in this work (EQ12) already included the other diagnostics housed in the port: Radial X-Ray Camera, GDC and Hard X-Ray Monitor inside the drawer 2, and Collective Thomson Scattering inside the drawer 3.

2. The resultant STEP simplified model (figure 2a) is introduced in the interface code MCAM [17] to be converted directly into the MCNP geometrical input. Often, part of the simplification of the engineering model can be carried out also *via* MCAM code (the “Split” tool and the Boolean operations are very useful to create void cells easily).

3. The .txt geometric MCNP input file of the Port Plug and the diagnostic generated by MCAM is then introduced in the global ITER MCNP model, C-LITE VERSION 1 RELEASE 131031 ISSUED 31/10/2013 (figure 2b). The model consists of a 40° regular sector, up to the bio-shield, with reflective boundary conditions at lateral sides of the sector.

4. The transport analyses are then performed using the Monte Carlo code MNC5 v.1.6 [18] and FENDL 2.1 [19] cross section data library to simulate the coupled neutron/photon transport. The neutron source specification corresponds to the standard 500 MW of fusion power at steady state with 400 MW of 14.1 MeV D-T neutrons. Parallel simulations have been carried-out using MPI on CIEMAT EULER cluster.

5. For the activation assessment of the optical components under the ITER fluxes in the corresponding positions, the ACAB code [20] and EAF2007 libraries [21] have been used.

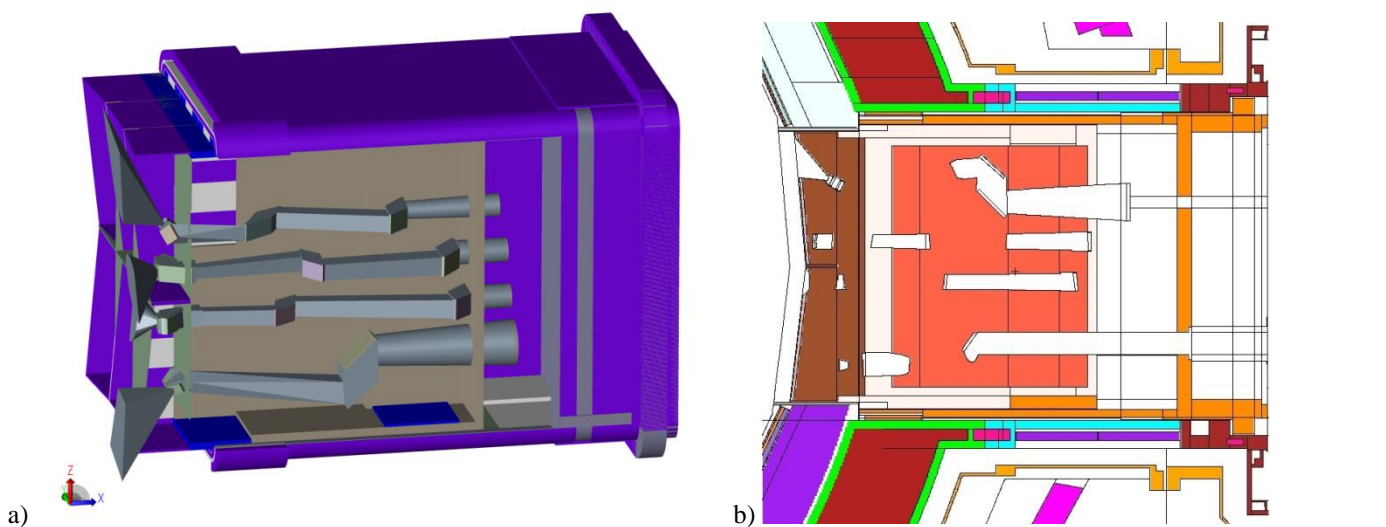


**Figure 2.** a) VIS/IR diagnostic components inside the EPP simplified for the neutronics purposes; b) neutronic MCNP model of the EPP and the diagnostic introduced in the global ITER MCNP C-LITE model.

## 4. Neutronic and Activation Analyses

### 4.1 Test to verify the silver usability as optical component for the interspace mirrors

Metals are opaque to all electromagnetic radiation on the low end of the frequency spectrum from radio waves, through infrared, the visible, and into about the middle of the ultraviolet radiation, while are transparent to high-frequency (x- and  $\gamma$ -ray) radiation. Most of the absorbed radiation is reemitted from the surface in the form of visible light of the same wavelength, which appears as reflected light. The reflectivity for most metals is between 0.90 and 0.95; some small fraction of the energy from electron decay processes is dissipated as heat. Since metals are opaque and highly reflective, the perceived color is determined by the wavelength distribution of the radiation that is reflected and not absorbed. A bright silvery appearance when exposed to white light indicates that the metal is highly reflective over the entire range of the visible spectrum. In other words, for the reflected beam, the composition of these reemitted photons, in terms of frequency and number, is approximately the same as for the incident beam. Aluminum and silver are two metals that exhibit this reflective behaviour (figure 3).

For the mirrors of the VIS/IR diagnostic inside the Interspace area a silver coating has been considered due to the high reflectance (0.95-0.98) of Ag in a wide range of wavelengths (400- 20.000 nm). In section 4.3, an assessment of Al coating, considered for the doglegs mirrors inside the Port, will also be presented.

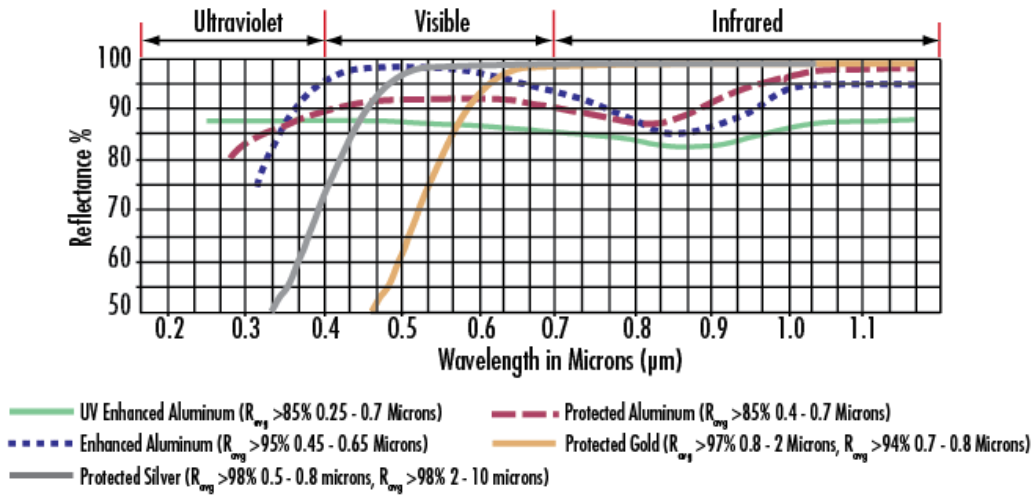


**Figure 3.** Metallic Mirror Coating Reflectance Curves - Theoretical reflectance rises gradually through  $10\mu\text{m}$  [22].

According to older examples on the usability of silver as brazing material performed among Remote Handling tasks [23], the use of silver requires prior acceptance from ITER and in any case it is required to assess the specific case. For this reason we have proceeded to analyse the possibility of using silver as coating material by performing, as preliminary assessment, the calculation of the surface gamma dose rate through the ACAB activation code.

The input data from ITER are the neutron fluxes in the different last positions, inside the Port Plug, of the 4 optical paths (positions U10, R10, L10 and D8 of figure 1a). These positions correspond to the vacuum window just before the Interspace area but, since the mechanical environment in the Interspace is not still completely defined, the neutron flux in these positions can be taken conservatively as representatives of what occurs in the Interspace. According to the ITER data, the values of the fluxes are within  $1.3\text{e}8 - 9.5\text{e}8 \text{ n/cm}^2\text{s}$  range [8].

Furthermore, as the life time during which the diagnostic should operate is still uncertain, it was established to simulate three irradiation conditions: 1FPY (equivalent to much more than 20 pulsed years, ITER end of life – EOL - according to the safety scenario SA2 of ITER [24]), 6 months (19 pulsed years) and 1 month at full power (8 pulsed years).

The results of surface gamma dose rate under the different irradiation histories and for the minimum and maximum neutron fluxes are summarized in table 1, giving values at different times after the shutdown. The results show that the safety criteria: “the dose rate at  $10^6 \text{ s}$  after shut-down shall be less than  $100 \mu\text{Sv/hr}$ ” (i.e., ALARA guideline for allowing radiation workers hands-on access) [25] is not observed even in the best conditions, namely, using the lower neutron flux in the best window position ( $10^8 \text{ n/cm}^2 \text{ s}$ ) and only 1 full power month of irradiation time. This is essentially caused by the very long life daughter isotopes produced through Ag activation.

**Table 1.** Results of surface gamma dose rate at different times after the shutdown, caused by an irradiation of 1 year/6 months/1 month (full power) for the two maximum and minimum values of neutron flux in the last position of the 4 optical paths inside the Port Plug. The values (given in Sv/hr) show that the safety (ALARA) criterion is not fulfilled also in the best conditions (lesser neutron flux and lesser irradiation time).

Neutron flux		<b>1e9 n/cm<sup>2</sup> s</b>			<b>1e8 n/cm<sup>2</sup> s</b>
Irradiation time		1 year	6 months	1 month	1 month
<b>Time after shutdown</b>		<b>Surface gamma dose rate</b>			
0 s	shutdown	2.79E-02	2.59E-02	2.17E-02	2.17E-03
4.24E+05 s	5 days	1.81E-02	1.61E-02	1.20E-02	1.20E-03
<b>1.05E+06 s</b>	<b>12 days</b>	1.04E-02	8.41E-03	5.01E-03	<b>5.01E-04</b>
3.15E+07 s	1 year	2.16E-03	1.41E-03	2.74E-04	2.74E-05

Although the contact dose obtained for the silver is high, since the amount of silver employed as coating for the optical components will be very low, the potential use of silver remains possible. In order to verify it, residual dose rate calculation is being performed.

## 4.2. Assessment of the irradiation time required in a Co-60 facility to provide an equivalent gamma dose then the accumulated in ITER at the vacuum window

Another of the needs and aims of the project is to test the possible optical materials under ITER-like conditions, namely in terms of both neutrons and gamma irradiation and also environmental conditions (temperature, humidity). Up to date the material selected for the vacuum window is sapphire ( $\text{Al}_2\text{O}_3$ ).

Sapphire is not only highly transparent to wavelengths of light between 150 nm (UV) and 5500 nm (IR), but is also extraordinarily scratch-resistant. Its key features are:

- Very wide optical transmission band from UV to near-infrared, (0.15-5.5  $\mu\text{m}$ )
- Significantly stronger than other optical materials or standard glass windows
- Highly resistant to scratching and abrasion (9 Mohs scale, the 3rd hardest natural substance)
- Extremely high melting temperature (2030  $^{\circ}\text{C}$ )

Taking advantage of these performances it has been established to test its behaviour under gamma, irradiating the material in a  $^{60}\text{Co}$  facility called Nayade, emplaced at CIEMAT, under the specific contract SG07 of grant F4E-FPA-407 funded by Fusion For Energy.

With the aim to define the irradiation campaign of sapphire specimens in the  $^{60}\text{Co}$  gamma facility, it has been determined the irradiation time required in the Nayade to provide the equivalent gamma dose that the sapphire vacuum window would receive at the End-of-Life (EOL) in ITER. Being conservatives, a lifetime of 20 pulsed years has been established for the diagnostic (and thus for the window) that is equivalent (SA2 irradiation scenario) to 195.6 full power days (FPD), namely 16899840 s. The gamma spectrum [26] for the windows located at the closure plate of the EPP12 has been used. The spectrum is shown in figure 4 and the total gamma fluence rate (averaged for the 3 views, ULR) is  $3.13\text{e}8$  ph/cm $^2$ s. The gamma dose rate in the Nayade provided by  $^{60}\text{Co}$  (CIEMAT data input) is 1.6 Gy/s.

In order to calculate the energy deposition in sapphire ( $\text{Al}_2\text{O}_3$ ) induced by photon, the spectrum, in the considered location, has been used as photon source in the center of a spherical sapphire sample small enough to not modify the photon spectrum along such a sphere. Results of fluence (MCNP tally F4), energy deposited (MCNP tally F46) and integrated dose over the ITER lifetime are summarized in table 2. With these data it follows that the equivalent irradiation time required for achieving the same gamma dose in the Nayade than in ITER, is less than 7 hours.

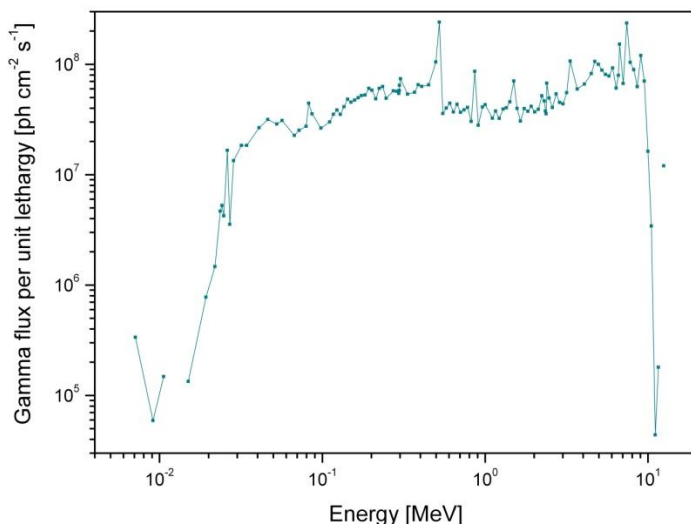


**Figure 4.** Gamma spectrum in the vacuum window used to determine the irradiation time (inside the  $^{60}\text{Co}$  gamma Nayade) of the sapphire material of which the window could be done.

**Table 2.** Results of gamma fluence (F4), energy deposited (F6) and integrated dose over the ITER lifetime for the sapphire vacuum window. The required irradiation time in the Nayade of  $^{60}\text{Co}$  to reach the same ITER dose after 20 pulsed years is given.

Magnitude	Unit	Values
Photon fluence rate	ph/cm $^2$ s	3.13E8
Photon fluence	cm $^2$	2.86E-1
Energy deposited	MeV/gr	1.296E-2
Gamma Dose rate	Gy/s	2.28E-3
Irrad. Time ITER	s	16899840
Integrated Dose	Gy	3.85E4
Required irradi. time		6.68 (hours)

### 4.3. Neutron and gamma dose rate maps for test and material choice of the optical components inside the Port Area

The experimental tests established under the SG07 in principle will be held in the  $^{60}\text{Co}$  Nayade facility located in CIEMAT (Spain) for gamma irradiation, as said before, and in the SCK•CEN BR2 reactor at Mol (Belgium) for neutron irradiation. To allow consistent specifications for the experimental campaigns with neutrons and gamma, needed for the selection of the optical materials, new assessments are under investigation as the neutron and gamma dose rate maps in the whole Port and Interspace areas during operation in the different materials considered for mirror and lenses.

Up to now, the analyses of the neutron and gamma dose rates we have performed are only in the Port area. In order to prevent neutron streaming along the optical lines (which could result in unacceptable radiation levels and activation of materials increasing the residual dose rate in the Interspace), the optical components in the Port area must be arranged in labyrinths (e.g. a dog-leg) interspersed with radiation shielding. However, combining the labyrinths for several optical paths in the limited space available will imply a difficult implementation of an effective shielding. In the following analyses to enable an efficient shield, the space left by the optical paths is filled with B<sub>4</sub>C powdered.

The materials for the optical system have to show good transmittance for lenses and reflectance for mirrors in the VIS (0.4-0.7 μm) and IR (3-5 μm) ranges, hardness against the environment neutron and gamma radiations, and compatibility with the operational temperature. In addition it would be an advantage if the lenses had limited reflection losses as this would reduce the need for optical coating for both wavelength ranges. Finally the materials chosen must not present major inconvenient such as deformability, birefringence, low polishing feasibility, etc. These constraints brought together reduce severely the possibilities for the material choice.

For the moment the analyses of the neutron and gamma dose rates have been centered on the following materials considered for the dogleg mirrors inside the Port Plug: Suprasil® (synthetic fused silica, SiO<sub>2</sub> amorphous), Boostec® SiC, ULE® (90% SiO<sub>2</sub> and 10% TiO<sub>2</sub>) and Bulk Al alloy (baseline 6061 T6), as substrates, and Nb<sub>2</sub>O<sub>5</sub>/SiO<sub>2</sub> and Al+SiO<sub>2</sub>, as coatings. The main characteristics and some of the applications of these materials are described as follows.

Silicon dioxide (SiO<sub>2</sub>) occurs naturally as sand or rock, and when melted, the resulting product is called Fused Quartz. If the silicon dioxide is synthetically derived, the material is often called Fused Silica [27]. Fused silica is a very common and well characterized material. Because of its high UV, VIS and NIR transmittance, ability to rotate plane polarized light, high damage threshold and resistance to scratching it is used in many optical applications as laser beam splitters, polarizing optics, prisms, windows, and lenses in the ultraviolet. The optical grade material is featured by the highest possible transmittance throughout the range of 190-2900 nm. The low thermal expansion coefficient makes it ideal for mirrors and optical flats. It is used for viewing windows, being transparent to wavelengths from around 0.2 to 3.5 μm. In our analyses a pure composition has been used with 2.2 g/cm<sup>3</sup> density.

Boostec® SiC [29] has been extensively used in space and laser technology, showing high thermal stability and insensitivity to radiation in the space environment. Its excellent mechanical properties permit the production of all optical benches and telescopes: mirrors, structure, and focal plane elements. These instruments are insensitive to temperature variations without any temperature control. Ground-based observatories profit from the same remarkable properties of Boostec® SiC, especially for their mirrors or their adaptive optics. The SiC technology permits the realization of lighter mirrors, with high dynamic flatness, low inertia and therefore very agile, for sighting systems, high speed laser scanners and LIDARS. For Boostec® SiC we consider 3.15 g/cm<sup>3</sup> density and a composition with only the main elements: 0,99 SiC and 0,01 B (wt. fractions).

Ultra low expansion ULE® glass [30][29] contains silica and less than 10% titanium dioxide. It has a very low coefficient of thermal expansion that makes it very resistant to high temperature thermal shock. ULE has been made by Corning since the 1960s but is still very important to current applications. There are many applications for ULE, but by far the most common has been for mirrors and lenses for orbiting telescopes and terrestrial bound telescopes, examples of which are the well-known Hubble space telescope and the Gemini telescope. The composition here considered is 0.9 SiO<sub>2</sub> and 0.1 TiO<sub>2</sub> (wt. fractions) with a density of 2.21 g/cm<sup>3</sup>.

Aluminum 6061-T6 is a precipitation hardening aluminum alloy, containing magnesium and silicon as its major alloying elements. It has good mechanical properties and exhibits good weldability. It is one of the most common alloys of aluminum for general purpose use. The composition used, in agreement with [31] is Al 0,97 - Cr 0,003- Cu 0,003- Fe 0,005- Mg 0,01- Mn 0,001- Si 0,005- Ti 0,001- Zn 0,002 (wt. fractions) and with 2.7 g/cm<sup>3</sup> density.

The use of niobium pentoxide (Nb<sub>2</sub>O<sub>5</sub>) increases the refractive index of optical glasses [32]. When it is added to the glass during the production of optical lenses, the lenses are lighter, thinner and demonstrate greater resilience. Adding niobium pentoxide to spherical lenses allows the number of lenses in optical elements to be reduced, which makes the components lighter and smaller. Nb<sub>2</sub>O<sub>5</sub> has been identified as being capable of reversible and rapid coloration in the presence of intercalating ions such H<sup>+</sup> and Li<sup>+</sup> ions. It has been reported that this phenomenon can modulate the Nb<sub>2</sub>O<sub>5</sub> optical transmission from a quasi-transparent state (T ~ 85%) to less than T ~ 10% in the ultraviolet (UV), visible or near infrared (IR) range. The refractive index value of Nb<sub>2</sub>O<sub>5</sub> has been reported to be in the order of 2 to 2.3 [33]. The composition considered in our assessments is stoichiometric pure composition with 4.47 g/cm<sup>3</sup> density. The neutron and thermal tests [35] showed that Nb<sub>2</sub>O<sub>5</sub>/SiO<sub>2</sub> coating is enough resistant to ITER-relevant conditions and can be recommended for ITER application.

Others materials initially considered, as the mirrors coated with TiO<sub>2</sub>/SiO<sub>2</sub> cannot be used in ITER due to reflectivity degradation at temperatures over 200 °C.

For the 5 main materials just mentioned, SiO<sub>2</sub>, SiC, ULE, Al alloy and Nb<sub>2</sub>O<sub>5</sub>, first results have been obtained about the neutron and gamma dose rates, in the whole Port area and considering the present optical path design, as maps distributions by using the “mesh tally” capability of MCNP5. According to the analyses performed, the three materials based on Silicon - SiO<sub>2</sub>, SiC and ULE - present very similar behaviour in terms of both neutron and gamma dose rates, thus only the results concerning SiO<sub>2</sub> are presented hereinafter. Thus, for the 3 optical materials: Al (1), Nb<sub>2</sub>O<sub>5</sub> (2) and SiO<sub>2</sub> (3), detailed results are presented for both

neutrons and gamma dose rate maps in radial-poloidal sections (figures 5 and 7, showing the four view paths together) as well as in radial-toroidal sections (figures 6 and 8, concerning only the values around the Right View system).

According to the results of neutron dose rate of figures 5 and 6, the lower values are shown when Aluminum is considered for the optical components.  $Nb_2O_5$  also give low neutron dose rate values. Materials based on Silicon present very similar results being the highest. It means that the time required to irradiate with neutrons (for example in the SCK•CEN BR2 reactor) will be longer for Si-based materials. In the maps representing the 3 materials together (down-left) it is possible to observe that the same ranking order (1, 2 and 3) is repeated in the different pieces of the 4 optical paths.

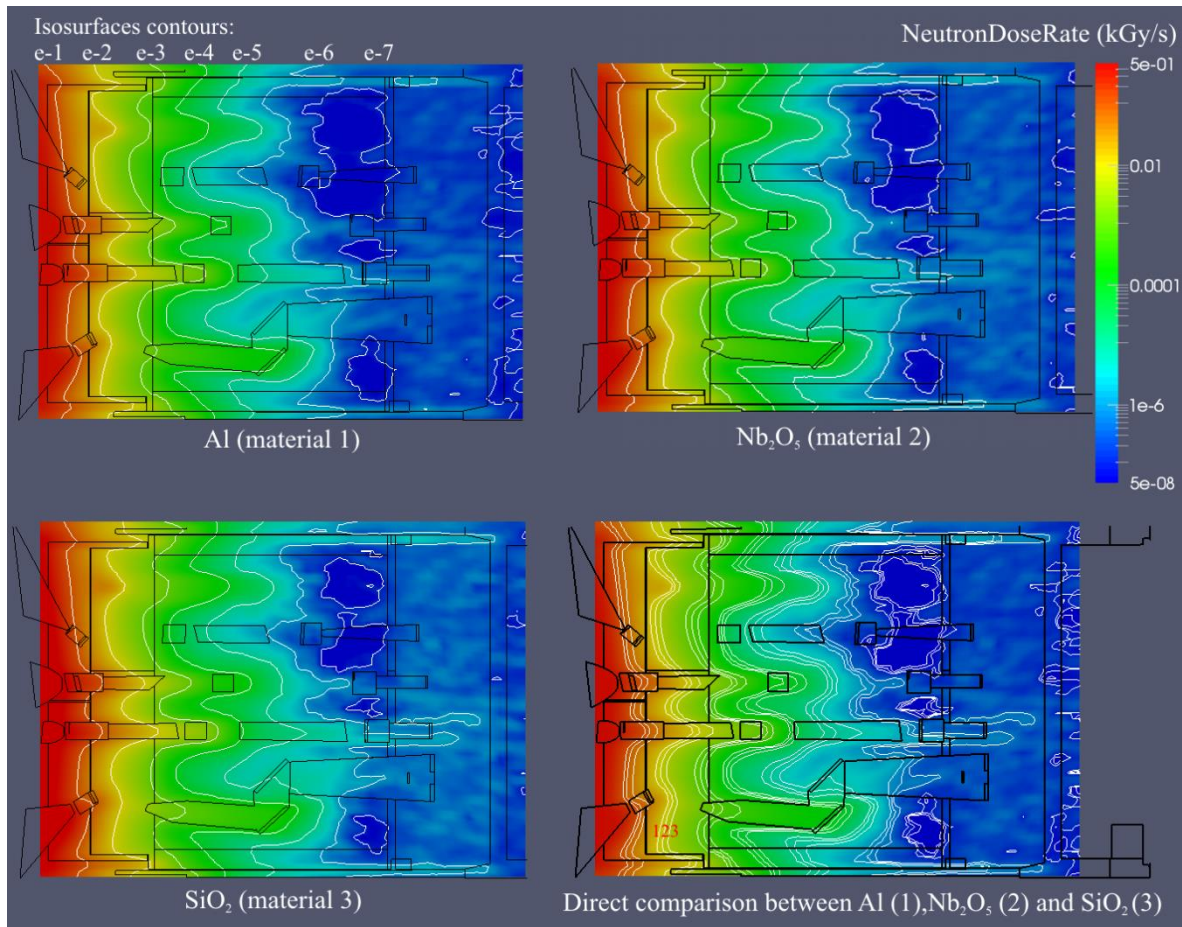


**Figure 5.** Neutron Dose Rate (in  $kGy/s$ ) in the 4 optical paths of the VIS/IR diagnostic system of the EP (radial-poloidal maps) for each of the three materials: Al (1),  $Nb_2O_5$  (2) and  $SiO_2$  (3) and a direct comparison between them overlapping the contours values produced in the three cases.

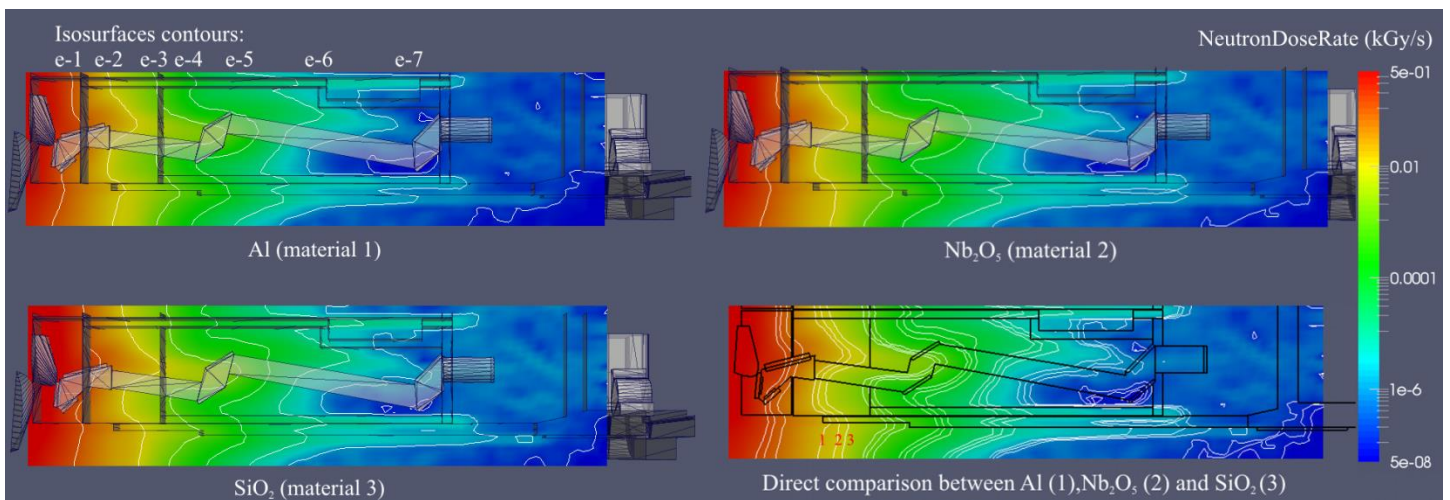


**Figure 6.** Neutron Dose Rate (in  $kGy/s$ ) in the Right View of the 4 paths of the VIS/IR diagnostic system of the EP (radial-toroidal sections) for each of the three materials: Al (1),  $Nb_2O_5$  (2) and  $SiO_2$  (3) and a direct comparison between them overlapping the contours values produced in the three cases.

On the contrary, concerning the results of the gamma dose rate shown in figures 7 and 8,  $SiO_2$  (as well as the other materials based on Silicon not represented) is now the material giving the lower gamma dose rate. Aluminum also presents very low values while  $Nb_2O_5$  generates the highest gamma dose rate. In order to determine the gamma irradiation test specifications it means that the

time required to irradiate with  $^{60}\text{Co}$  will be longer for  $\text{Nb}_2\text{O}_5$ . Again, in the maps representing the 3 materials together, the ranking order (now 3, 1 and 2) is repeated in the different positions (the optical components) of the 4 paths showing now an higher distance between the iso-surfaces of Al (1) and  $\text{SiO}_2$  (3) regarding the same surface values of  $\text{Nb}_2\text{O}_5$  (2).

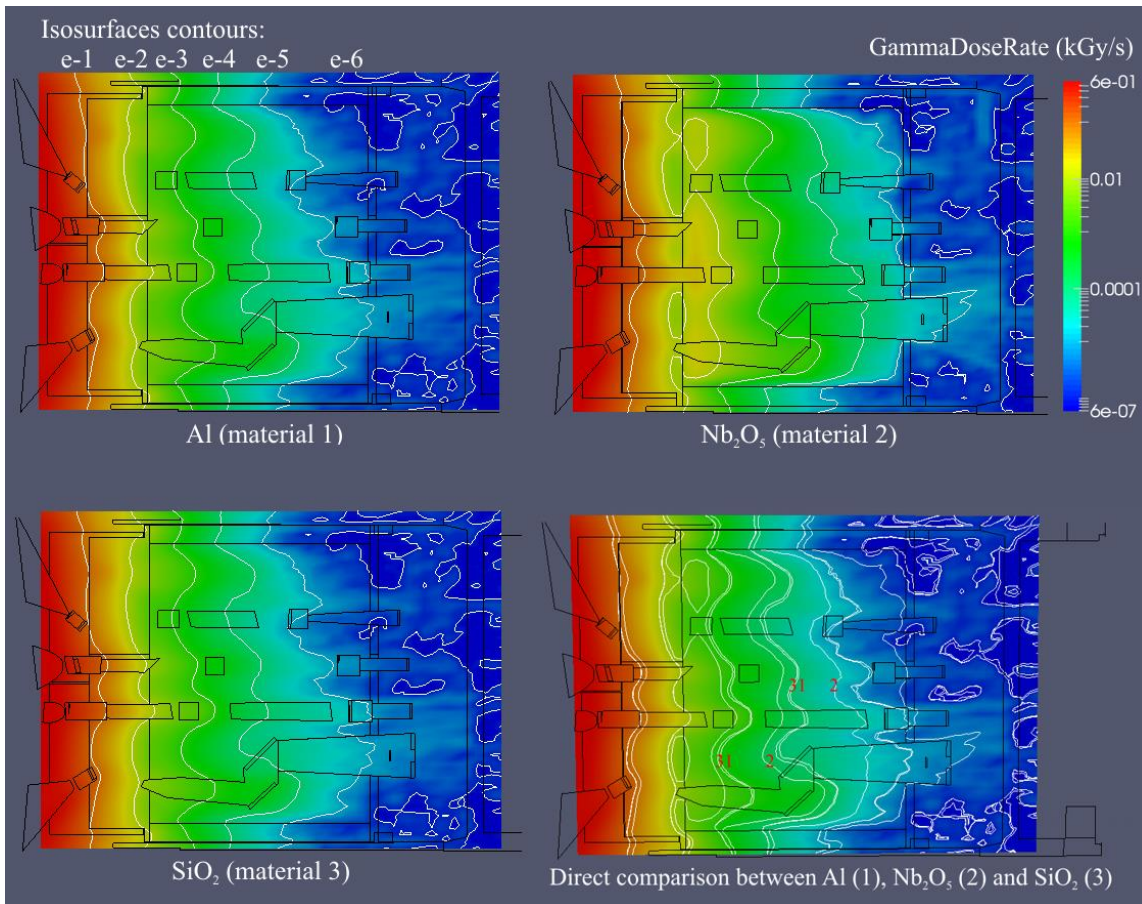


**Figure 7.** Gamma Dose Rate (in kGy/s) in the 4 optical paths of the VIS/IR diagnostic system of the EP (radial-poloidal maps) in each of the 3 different materials and comparison between them.

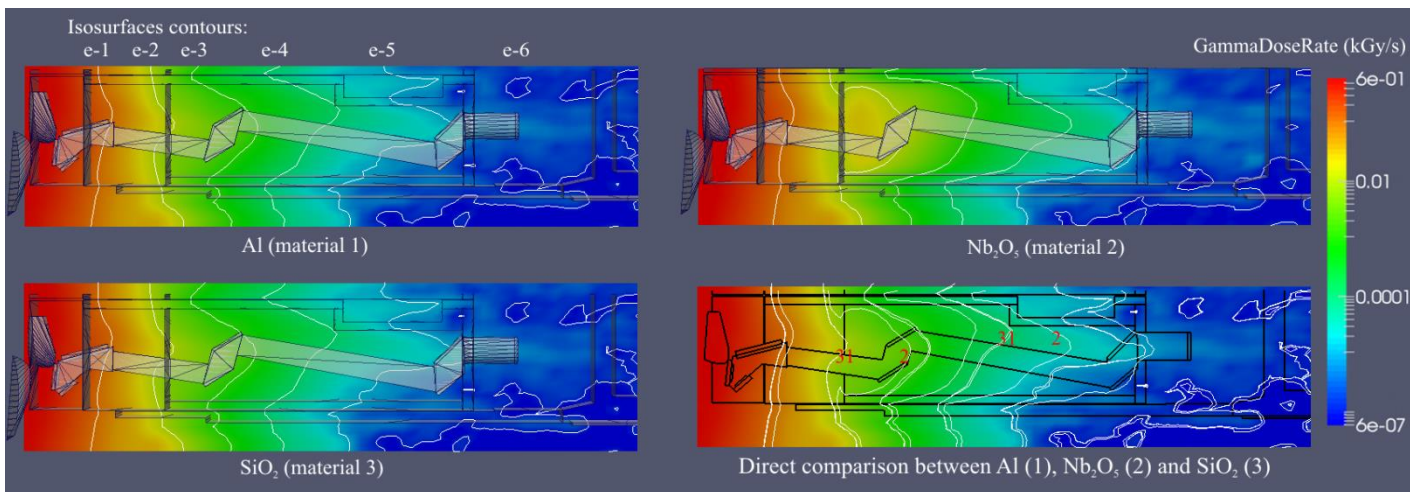


**Figure 8.** Gamma Dose Rate (in kGy/s) in the Right View (among the 4 optical paths) of the VIS/IR diagnostic system of the EP (radial-toroidal sections) in each of the 3 different materials and comparison between them.

As a result of the considerations here exposed the experimental campaigns will be determined using conservative assumptions i.e. the results of the material with longer irradiation time required ( $\text{SiO}_2$  for neutron irradiation campaign and  $\text{Nb}_2\text{O}_5$  for gamma irradiation campaign).

The maps shows great differences between the irradiation conditions required for the front end mirrors (from position 1 to 3 of figure 1a) respect to the vacuum windows (positions ULR10 and D8): there are 5 orders of magnitude of difference in the gamma dose rates and 6 orders in the neutron dose rates. This means that, differently from the result of 7 hours required to irradiate the sapphire vacuum window, for the first mirrors (positions 1-3), considering an optimistic assumption for the chosen material of  $\sim 1 \times 10^{-1} \gamma$  kGy/s, the irradiation time would be 33.95 years. Indeed the  $^{60}\text{Co}$  Nayade provides very low gamma dose rate making the irradiation campaign of the first mirrors unfeasible in this facility.

From the other side, according to the SCK data, the maximum gamma dose rate achievable in their facilities is 50kGy/h equivalent to 13,8 Gy/s (~10 times higher than the CIEMAT  $^{60}\text{Co}$  facility). It would reduce the irradiation time from 33.9 to 3.56 years, although continuing to be unviable. However, the irradiation facility has not been still fixed: others SCK/CEN facilities could allow achieving the target dose. In fact, BR1 reactor gives up to  $10^{11}$  n/cm<sup>2</sup> s, and BR2 gives higher fluxes, up to  $10^{15}$  n/cm<sup>2</sup> s, that seems could cover the experimental needs for both neutrons and gamma. Nevertheless, it is proposed to review the specifications of the irradiation experiments: by testing the conditions of mirrors not so highly exposed (intermediate mirrors only) or reaching doses lower than the expected EOL ITER dose.

Others assessments need to be done in order to give a complete evaluation of each material under activation/remote handling/damage point of view, among others. Furthermore, others studies are foreseen once the optical path, the components design and their materials will be newly established in order to determine if modifications or shielding improvements are required to keep the radiation limits posed by the material properties as well as the safety limits.

## 5. Conclusion and future developments

Recent progresses of the VIS/IR WAVS design have been presented focusing on the nuclear studies for assessment and test of material candidates for the optical components. Three main neutronic analyses have been performed: the first has given a preliminary evaluation of silver as covering material for the mirrors located in the 4 interfaces positions between the Port Plug and the Inter-Space area; the second, for testing materials purposes of the sapphire vacuum window, have allowed to assess the equivalent irradiation time required to achieve the same gamma dose in a  $^{60}\text{Co}$  gamma facility than in ITER, resulting less than 7 hours; and the third analysis, for a more precise assessment of the specifications of the irradiation campaigns under gamma and neutrons irradiation of the optical materials considered as substrate and coatings, have shown the need of a more powerful gamma facility than the  $^{60}\text{Co}$  Nayade in order to test the first mirrors under the EOL ITER conditions. Alternatively it has been proposed to reduce the specifications of the campaigns by simulating the conditions of the intermediate/doglegs mirrors only (avoiding the hardest experimental needs of the first mirrors) or considering shorter scenarios (not until ITER EOL). Based on the neutron and gamma dose rate results, it has been shown that among Silicon based materials, Aluminum and Nb<sub>2</sub>O<sub>5</sub> the highest irradiation times will be required to irradiate Si-based material for the neutron campaign and Nb<sub>2</sub>O<sub>5</sub> for the gamma.

Experimental tests under neutron, gamma and temperature ITER-like conditions will be made in order to follow with the choice of materials. Furthermore, the residual dose rate due to Ag coated mirrors will be analysed. The neutronic model of the Interspace area will be developed and the model for the Port area is being updated. Paramount issues are being tackled, relative to material choice and optomechanical difficulties due to the limited space available for this instrument in the ports, since many other diagnostics and services are also present. Thus further studies will be done to assess the shielding capability of the system and a shielding improvement could be required to keep the radiation limits posed by the material properties as well as the safety limits.

## Acknowledgements

This work has been partially founded by the EFDA Goal Oriented Training (GOT) Programme “WP12-GOT-4-DIAG”, Work Programme 7 and has been partially performed with the Fusion for Energy's collaboration and financial support, in the framework of grant F4E-FPA-407 SG01. The views and opinions expressed herein do not necessarily reflect those neither of Fusion for Energy nor of the ITER Organization. The authors wish to thank FDS Team, China, for providing the MCAM software.

## References

- [1] M. Davi et al., Progress of the ITER equatorial vis/IR wide angle viewing system optical design, *Rev. Sci. Instrum.* 79, 10F509 (2008)
- [2] S. Salasca et al., Development of equatorial visible/infrared wide angle viewing system and radial neutron camera for ITER, *Fus. Eng. Des.* 84, 1689 (2009)
- [3] R. Reichle et al., Defining the infrared systems for ITER, *Rev. Sci. Instrum.* 81, 10E135 (2010)
- [4] F. Moro et al., Neutronic analysis of the ITER Equatorial Port Plug 1, *Fus. Eng. Des.* 87 1224– 1229 (2012)
- [5] A. Serikov et al., Monte Carlo radiation shielding and activation analyses for the Diagnostic Equatorial Port Plug in ITER, *Fus. Eng. Des.* 87 690–694 (2012)
- [6] S. Salasca et al., Results of an integration study of a diagnostics port plug in ITER, *Fus. Eng. Des.* 88 602– 606 (2013)
- [7] R. Reichle et al., Concept development for the ITER equatorial port visible/infrared wide angle viewing system, *Rev. Sci. Instrum.* 83, 10E520 (2012)
- [8] A. Suarez et al., Load Specification for Visible/IR Wide Angle Viewing System in Equatorial Port Plug, ITER\_D\_BJHNF8, (2013)
- [9] R. Reichle et al., System Design Description Document DDD, Equatorial port visible/infrared wide angle viewing system, ITER\_D\_DCHGAP, (2013)
- [10] S. Yamamoto et al., Impact of irradiation effects on design solutions for ITER diagnostics, *J. Nucl. Mater.* 283-287 60-69 (2000)
- [11] A.E. Costley et al., ITER R&D: Auxiliary Systems: Plasma Diagnostics, *Fus. Eng. Des.* 55 331–346 (2001)
- [12] N. Baluc et al., Status of R&D activities on materials for fusion power reactors, *Nucl. Fusion* 47 S696–S717 (2007)
- [13] A. Ibarra, E.R. Hodgson, The ITER project: the role of insulators, *Nuclear Instruments and Methods in Physics Research B* 218 29–35 (2004)

- [14] A. Moroño, E.R. Hodgson, J. Nucl. Mater. 224 216 (1995)
- [15] A. Suarez, Neutronics Study of Diagnostic GEPP, ITER Internal Report D L9SVKT\_v1.2 (2014)
- [16] <http://www.spaceclaim.com/en/Products/Engineer.aspx>
- [17] Y. Wu, FDS Team, CAD-based interface programs for fusion neutron transport simulation, Fus. Eng. Des. 84 1987-1992 (2009)
- [18] X-5 Monte Carlo Team, MCNP—A General Monte Carlo N-Particle Transport Code, Version 5, Volume I, MCNP Overview and Theory, Los Alamos National Laboratory Report, LA-UR-03-1987, (2003)
- [19] D.L. Aldama, A. Trkov, FENDL-2.1: Update of an evaluated nuclear data library for fusion applications, Report INDC(NDS)-467, (2004)
- [20] J. Sanz, O. Cabellos, N. Garria-Herranz, ACAB-2008, ACTivation ABacus Code V2008, NEA Data Bank (NEA-1839), (2009)
- [21] R.A. Forrest, J. Kopecky, J.-Ch. Sublet, The European Activation File: EAF-2007 neutron-induced cross section library, UKAEA FUS 535, (2007)
- [22] <http://www.edmundoptics.com/technical-resources-center/optics/metallic-mirror-coatings/>
- [23] V. Queral, Feasibility assessment of in-vessel components connections for Remote Handling. EFDA\_D\_2LM5NS. Final Report for WP11-DAS-RH-04-04 (2012)
- [24] M.J. Loughlin, N.P. Taylor, Recommended Plasma Scenarios for Activation Calculations, ITER Internal Report ITER D 2V3V8G v 1.1, (2009)
- [25] H. Iida, V. Khripunov, L. Petrizzi, G. Federici, Nuclear Analysis Report (NAR), ITER Internal Report G 73 DDD 2 W 0.2, (2004)
- [26] JP Catalan, Neutron and gamma spectra for the Visible IR windows, ITER Internal Report PHQNB2, (2014)
- [27] [http://www.mt-berlin.com/frames\\_cryst/descriptions/quartz%20.htm](http://www.mt-berlin.com/frames_cryst/descriptions/quartz%20.htm)
- [28] [http://heraeus-quarzglas.com/media/webmedia\\_local/downloads/broschren\\_mo/Suprasil\\_UVL\\_synthetic\\_fused\\_silica.pdf](http://heraeus-quarzglas.com/media/webmedia_local/downloads/broschren_mo/Suprasil_UVL_synthetic_fused_silica.pdf)
- [29] [https://www.mersen.com/uploads/tx\\_mersen/22-boostec-sintered-SiC-mersen\\_09.pdf](https://www.mersen.com/uploads/tx_mersen/22-boostec-sintered-SiC-mersen_09.pdf)
- [30] Ken Hrdina, Production and properties of ULE® glass with regards to EUV masks, Presented at The International workshop on Extreme Ultraviolet Lithography, October 10-13, (1999)
- [31] <http://asm.matweb.com/search/SpecificMaterial.asp?bassnum=MA6061t6>
- [32] Rozina Abdul Rani et al., Thin films and nanostructures of niobium pentoxide: fundamental properties, synthesis methods and applications, J. Mater. Chem. A, 2, 15683, (2014)
- [33] C.-C. Lee, C.-L. Tien and J.-C. Hsu, Internal stress and optical properties of Nb2O5 thin films deposited by ion-beam sputtering, Appl. Opt., 41, 2043–2047 (2002)
- [34] X. Xiao et al., Structure and optical properties of sculptured Nb2O5 thin films by glancing angle deposition, Appl. Surf. Sci., 255, 2192–2195 (2008)
- [35] I. Orlovskiy et al., Broadband dielectric mirrors for optical diagnostics in ITER, Fus. Eng. Des. 88 1284–1287 (2013)